Supporting information for

Metal-organic-framework-derived porous 3D heterogeneous $NiFe_x/NiFe_2O_4$@NC nanoflowers as highly stable and efficient electrocatalysts for the oxygen-evolution reaction

Jia Zhao[1,#], Xu Zhang[1,#], Ming Liu[1], Yi-Zhan Jiang[1], Min Wang[1], Zhao-Yang Li[1,*], and Zhen Zhou[1,2]

[1]School of Materials Science and Engineering, Nankai University, 38 Tongyan Road, Haihe Educational Park, Tianjin 300350, P.R. China

[2]Tianjin Key Laboratory of Metal and Molecule Based Material Chemistry, Key Laboratory of Advanced Energy Materials Chemistry (Ministry of Education), Institute of New Energy Material Chemistry, Computational Centre for Molecule Science, Nankai University, Tianjin 300071, P.R. China

Email: zhaoyang@nankai.edu.cn

[#]J. Zhao and X. Zhang contributed to this work equally.

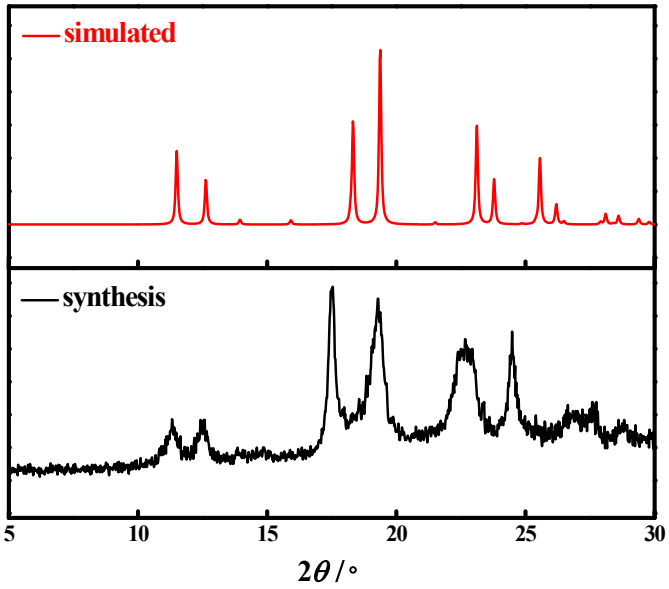

Fig. S1 The PXRD patterns of NiFe-HF.

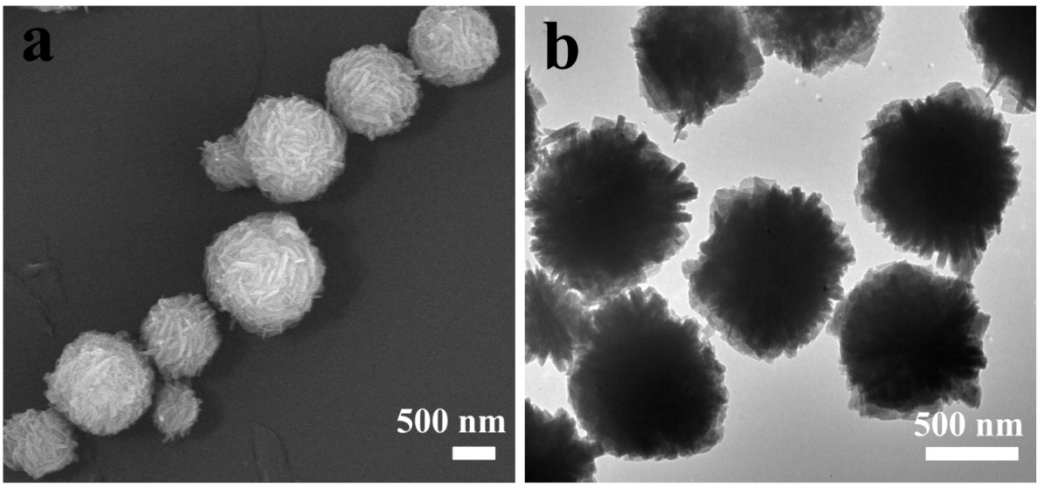

Fig. S2 The low-magnification SEM image (a) and corresponding TEM image (b) of NiFe-HF.

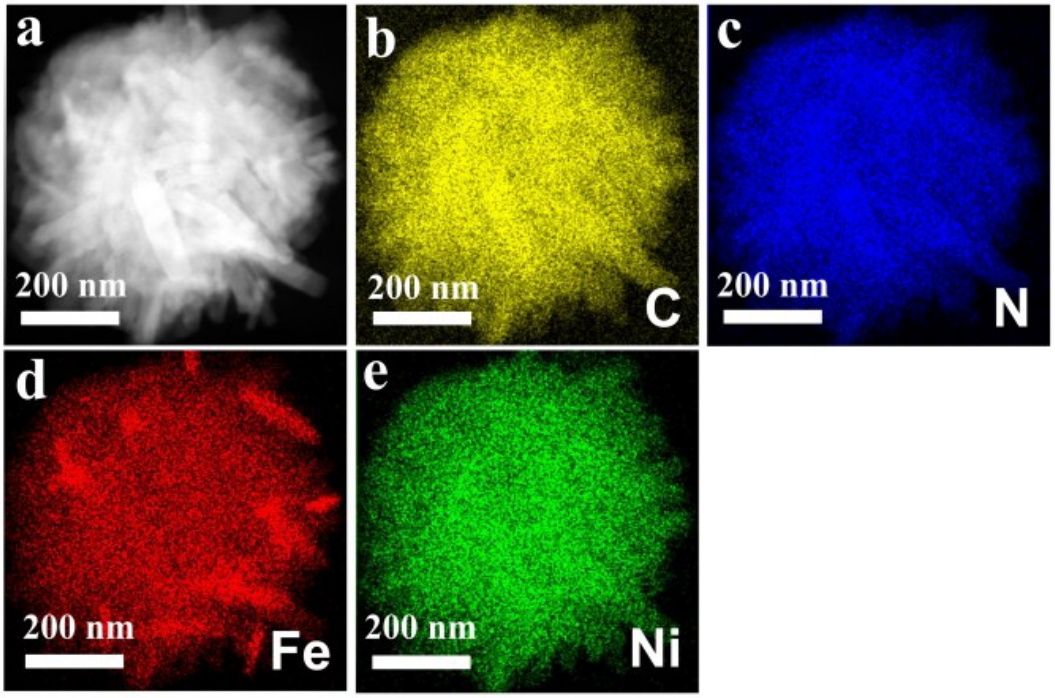

Fig. S3 The EDS-Mapping of single NiFe-HF nanoflower.

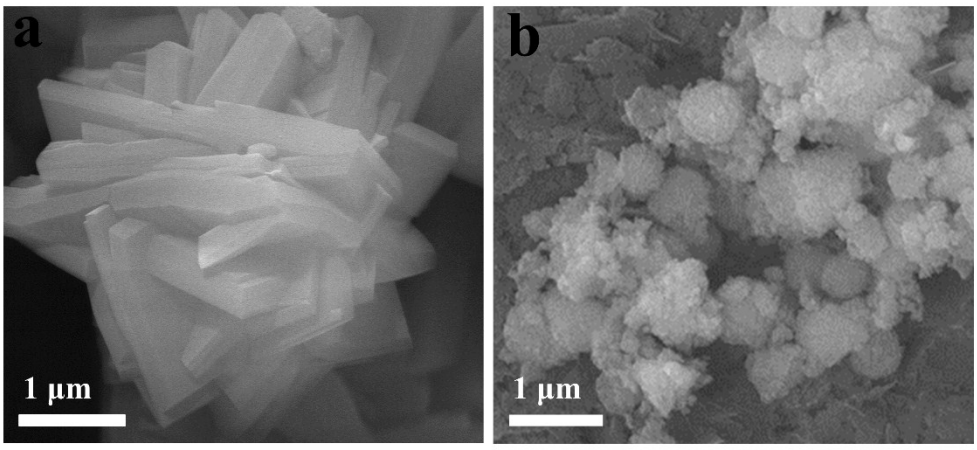

Fig. S4 (a) The SEM images of initial Hofmann MOFs (b) The SEM images of Hofmann MOFs, when the quality ratio of PVP and ascorbic acid is 10: 1.

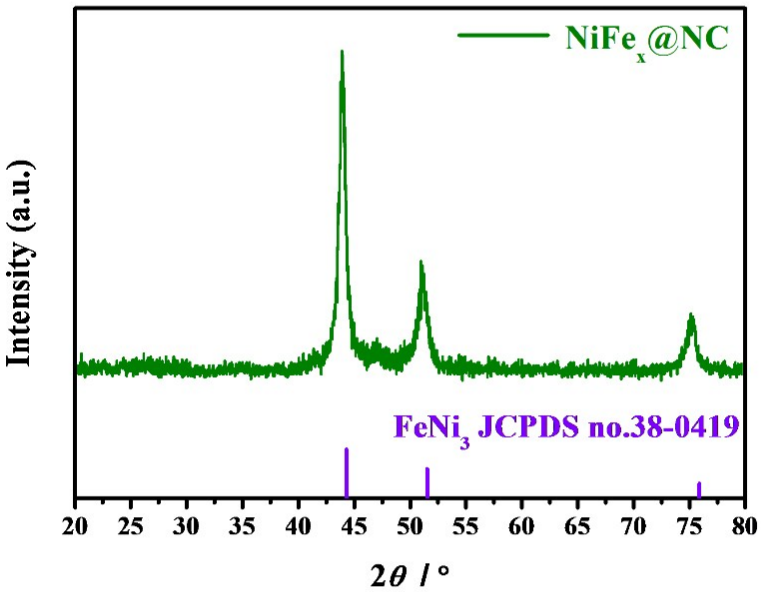

Fig. S5 The PXRD patterns of $NiFe_x$@NC.

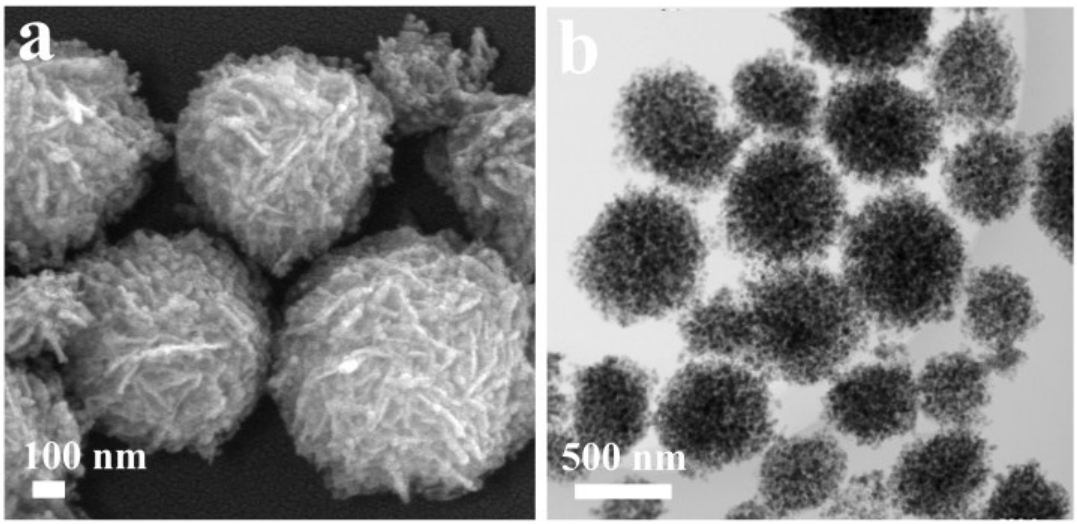

Fig. S6 The low-magnification SEM image (a) and corresponding TEM image (b) of $NiFe_x$@NC nanoflowers.

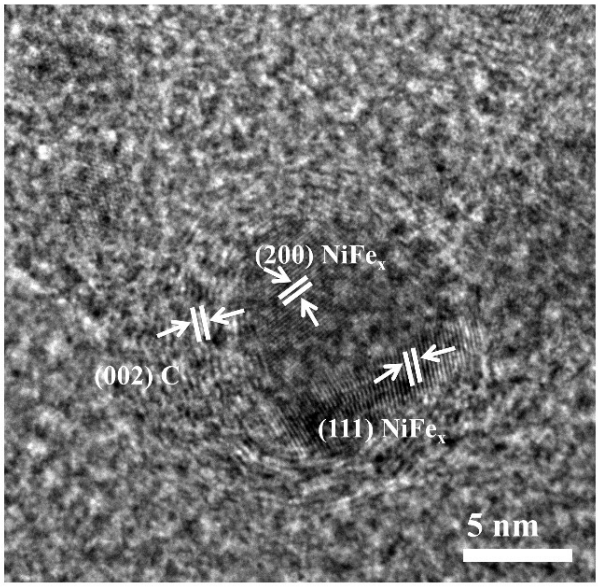

Fig. S7 HRTEM image of NiFe$_x$@NC nanoflower.

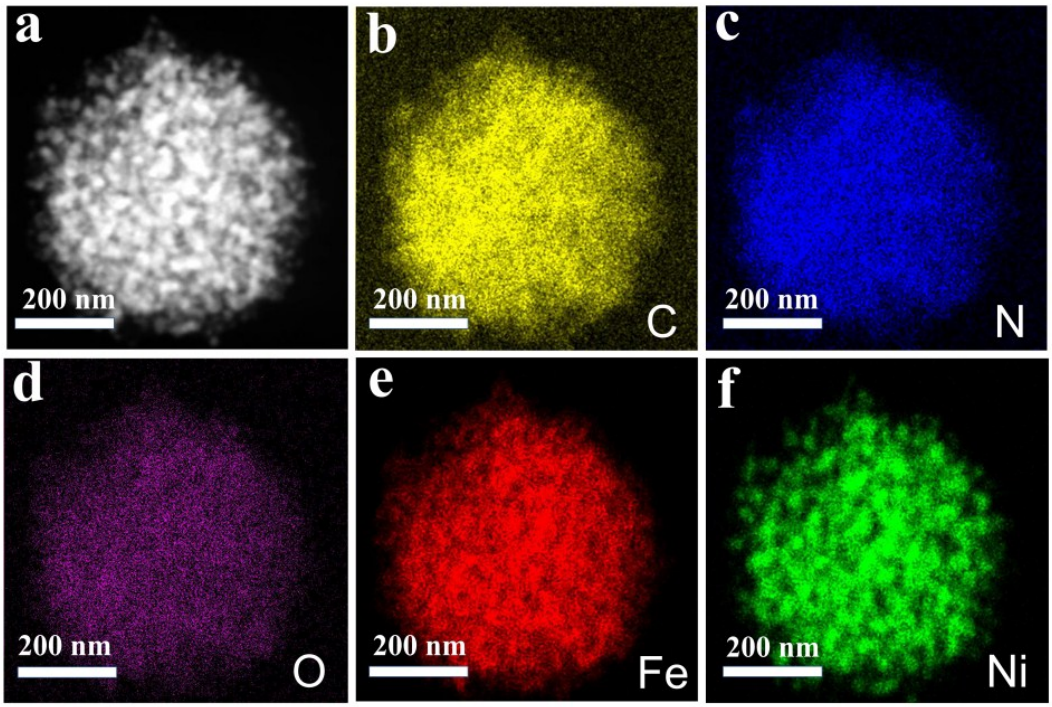

Fig. S8 The EDS-Mapping of single NiFe$_x$@NC nanoflower.

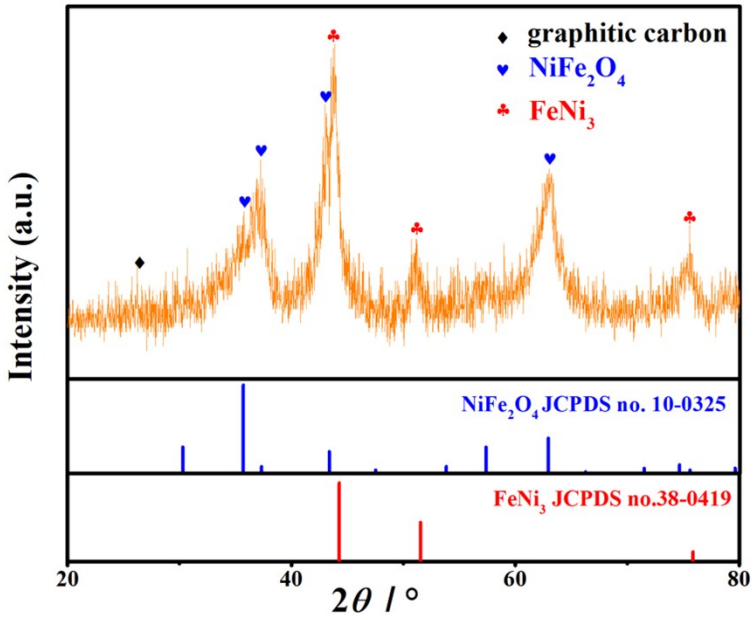

Fig. S9 The PXRD patterns of $NiFe_x/NiFe_2O_4$@NC.

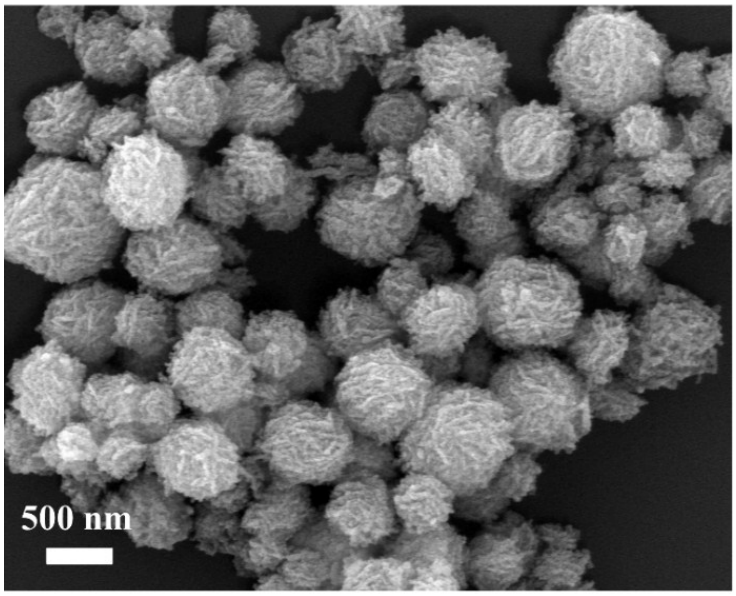

Fig. S10 The low-magnification SEM image of $NiFe_x/NiFe_2O_4$@NC.

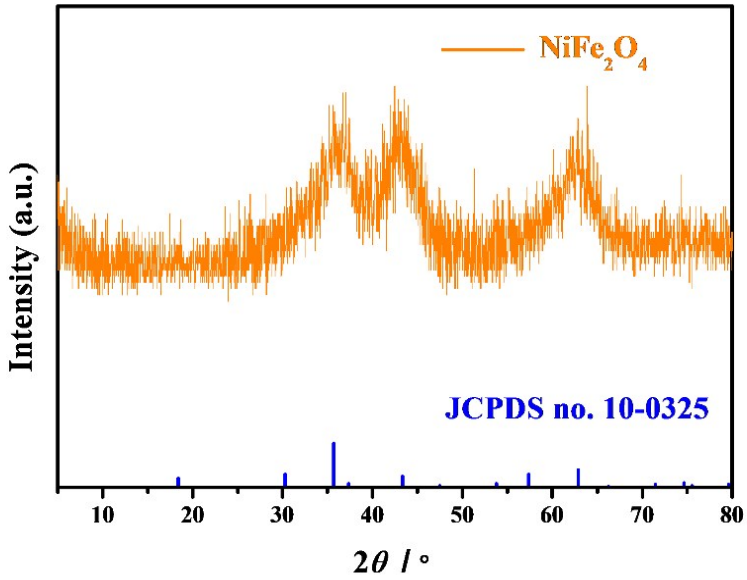

Fig. S11 The PXRD patterns of $NiFe_2O_4$.

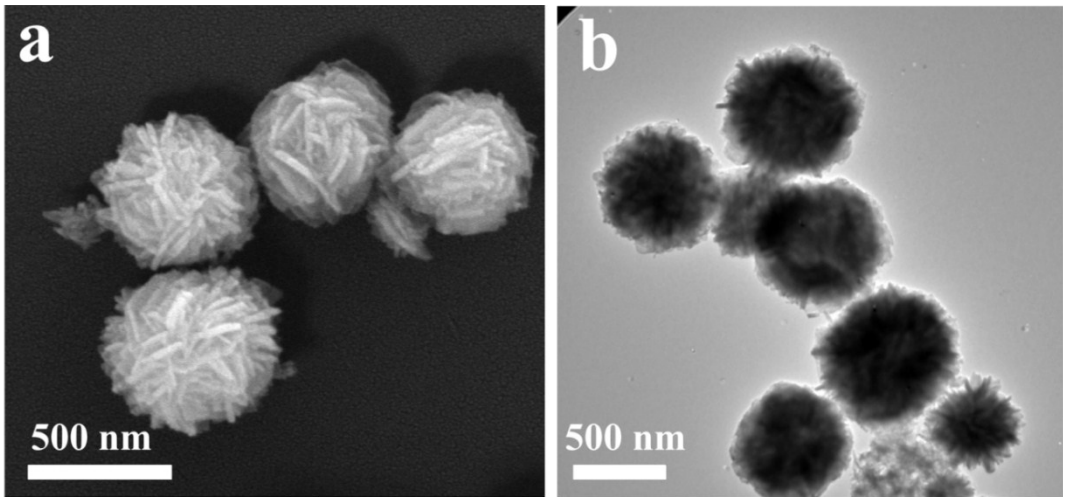

Fig. S12 The low-magnification SEM image (a) and corresponding TEM image (b) of $NiFe_2O_4$ nanoflowers.

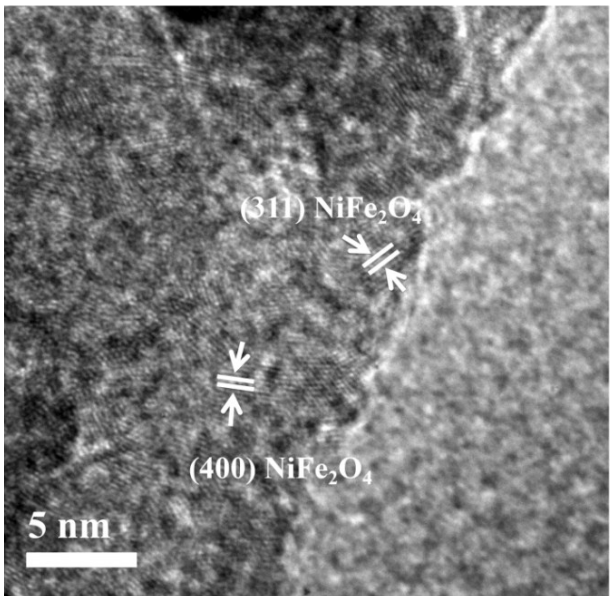

Fig. S13 HRTEM image of $NiFe_2O_4$.

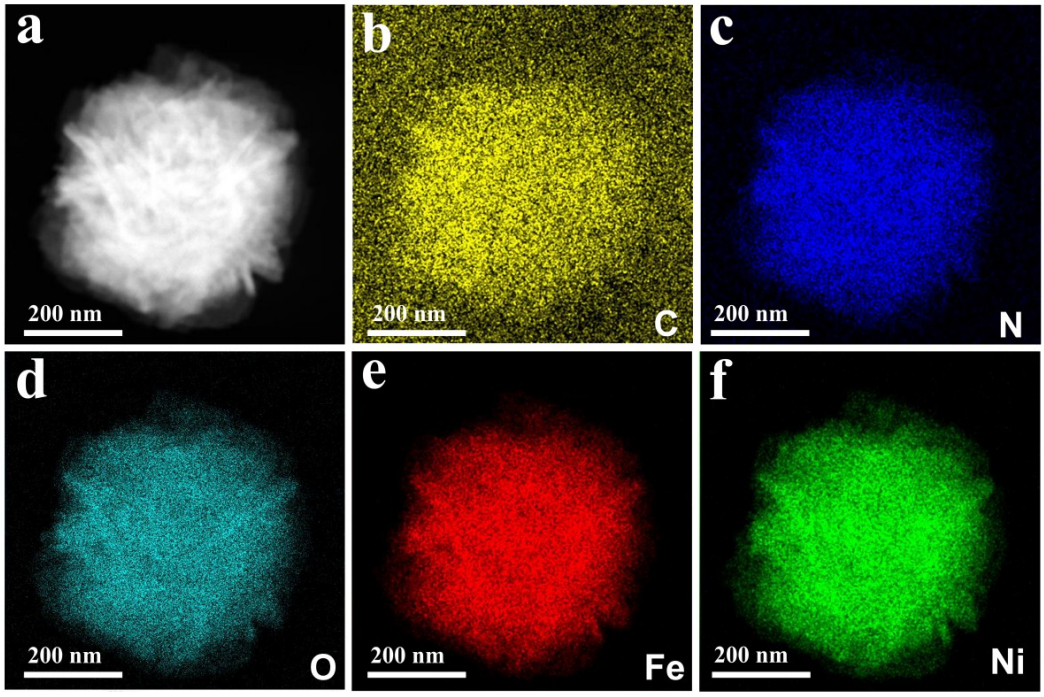

Fig. S14 The EDS-Mapping of single $NiFe_2O_4$ nanoflower.

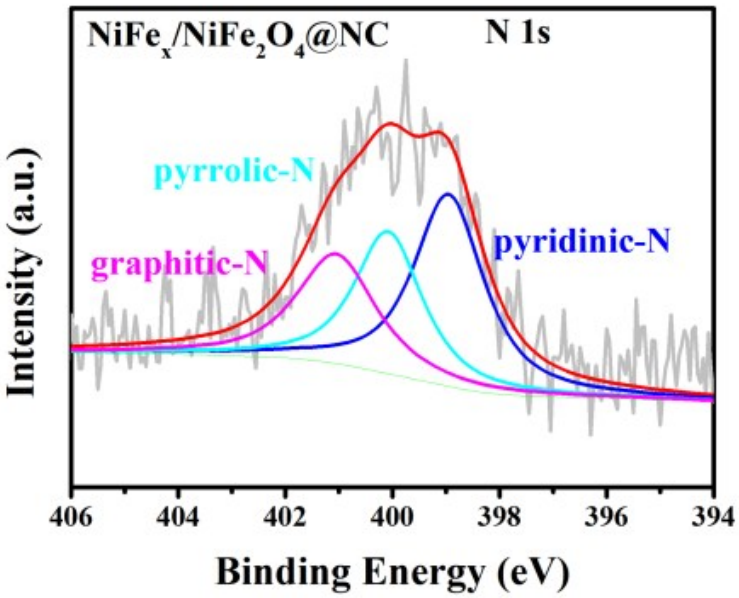

Fig. S15 The XPS N1s spectrum of $NiFe_x/NiFe_2O_4$@NC.

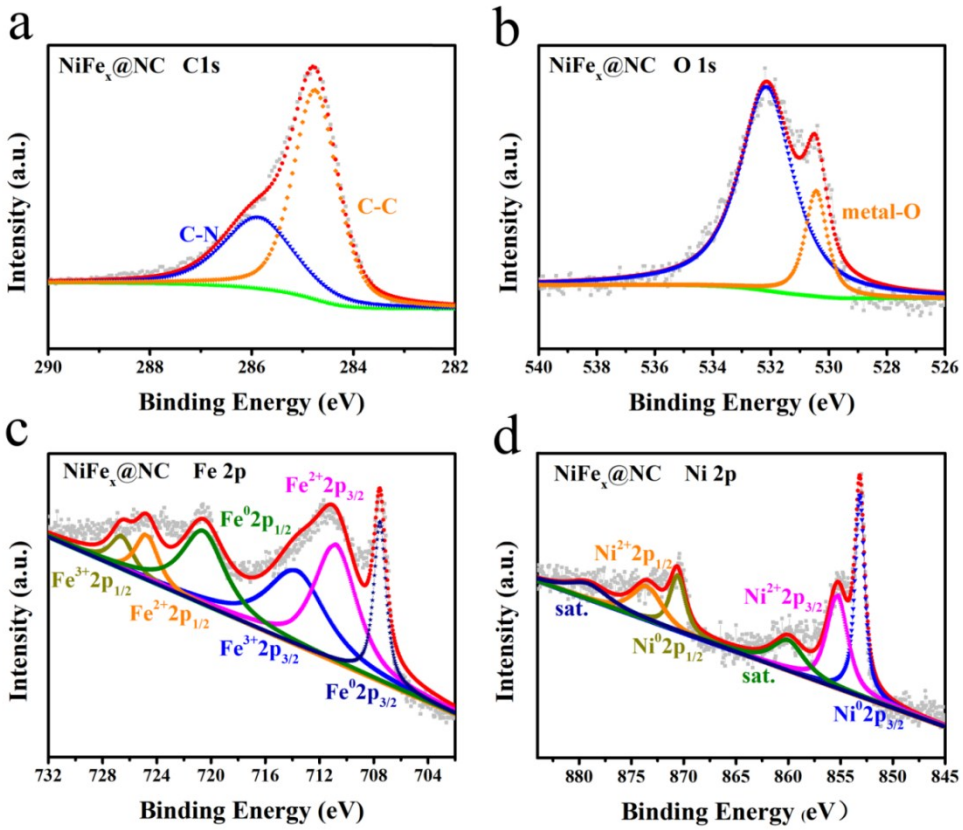

Fig. S16 The XPS C 1s, O 1s, Fe 2p and Ni 2p spectra of $NiFe_x$@NC.

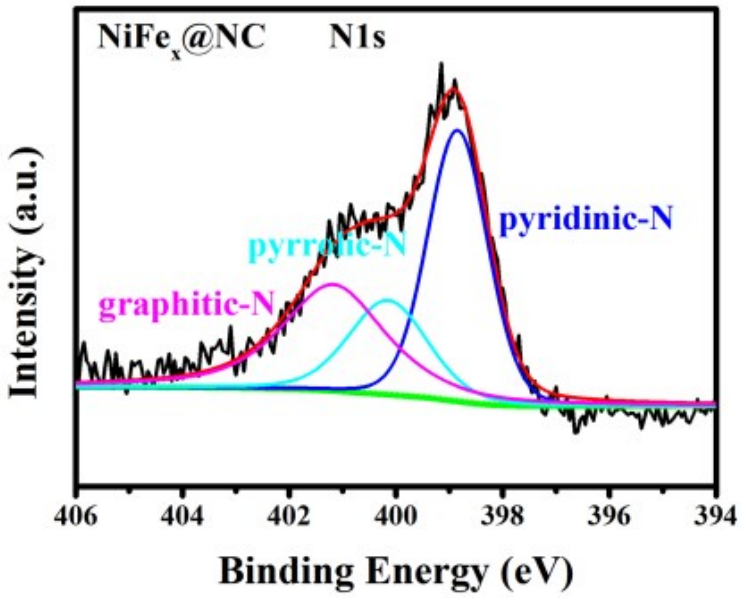

Fig. S17 The XPS N1s spectrum of $NiFe_x$@NC.

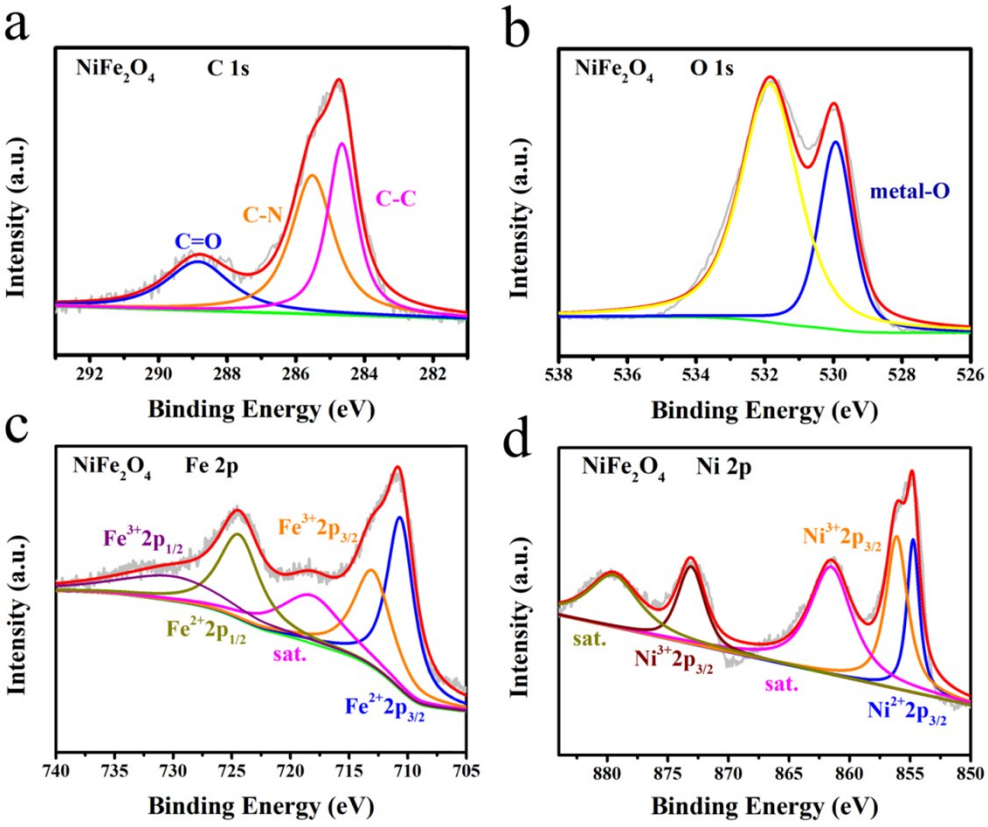

Fig. S18 The XPS C 1s, O 1s, Fe 2p and Ni 2p spectra of $NiFe_2O_4$.

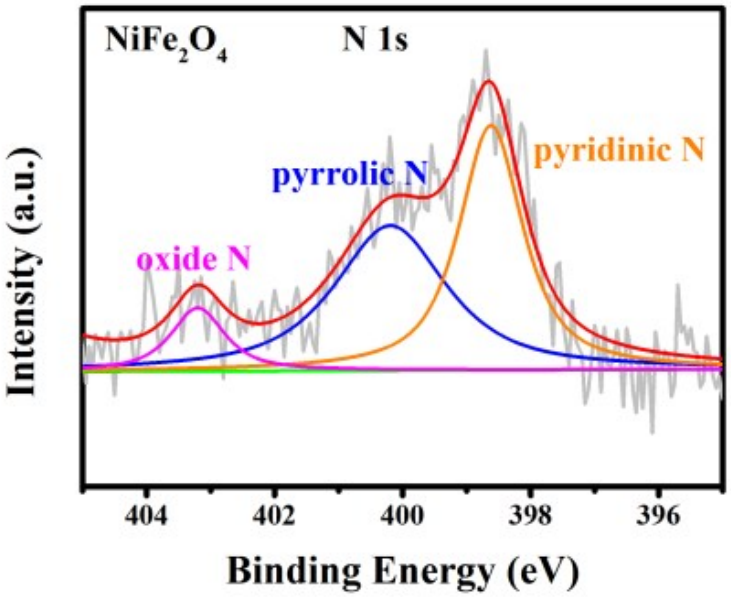

Fig. S19 The XPS N1s spectrum of $NiFe_2O_4$.

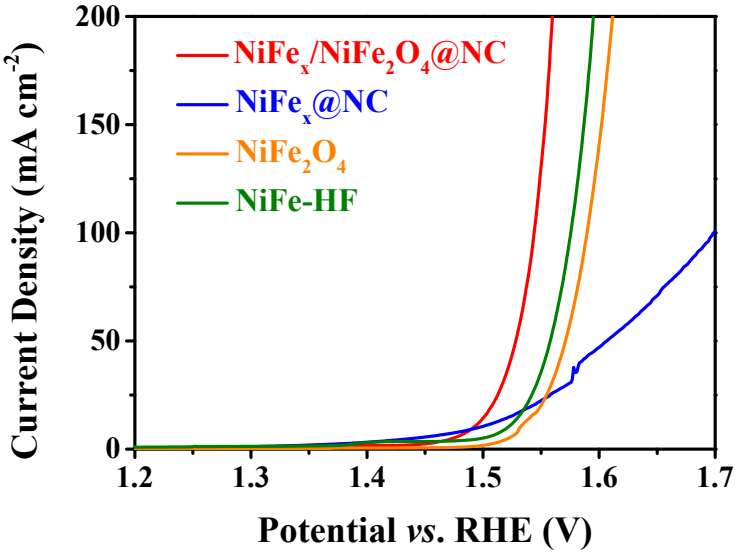

Fig. S20 LSV curves of $NiFe_x/NiFe_2O_4$@NC, $NiFe_x$@NC, $NiFe_2O_4$ and NiFe-HF.

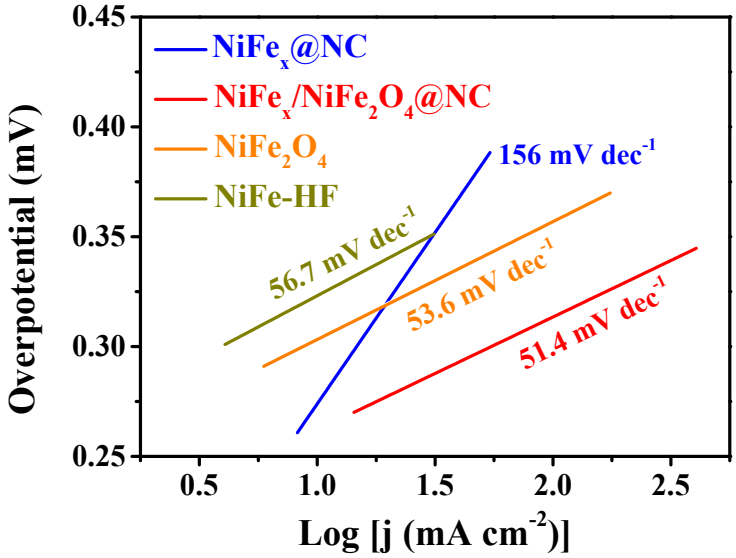

Fig. S21 Tafel plots of $NiFe_x/NiFe_2O_4$@NC, $NiFe_x$@NC, $NiFe_2O_4$ and NiFe-HF.

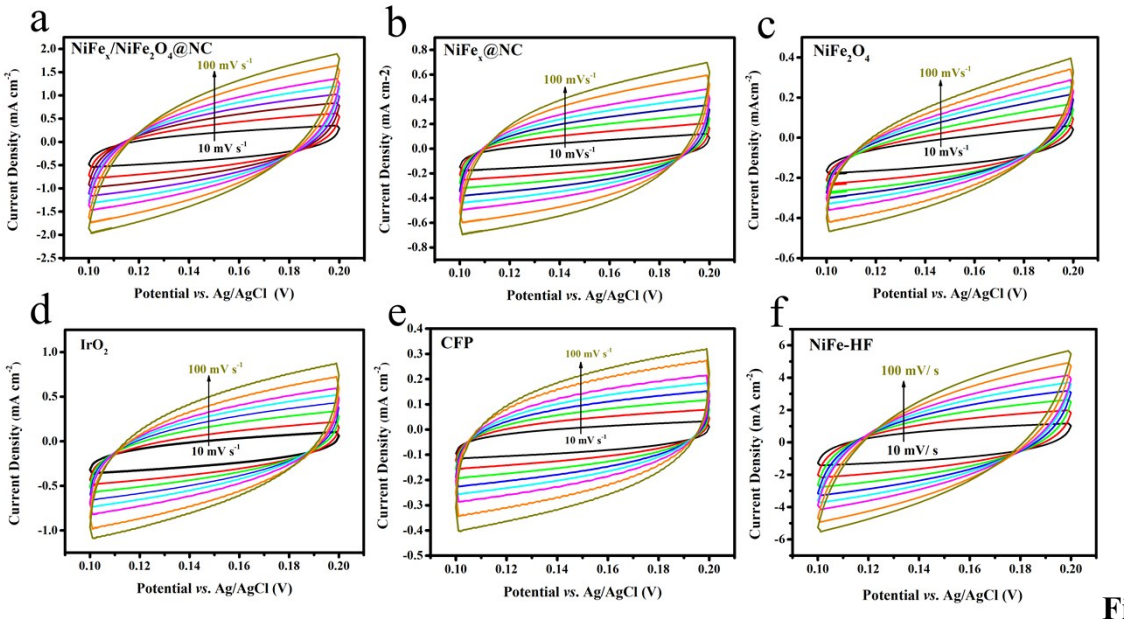

Fig. S22 CV curves from 1.11 to 1.21 V (*vs* RHE) of (a) $NiFe_x/NiFe_2O_4$@NC, (b) $NiFe_x$@NC, (c) $NiFe_2O_4$, (d) IrO_2, (e) CFP and (f) NiFe-HF.

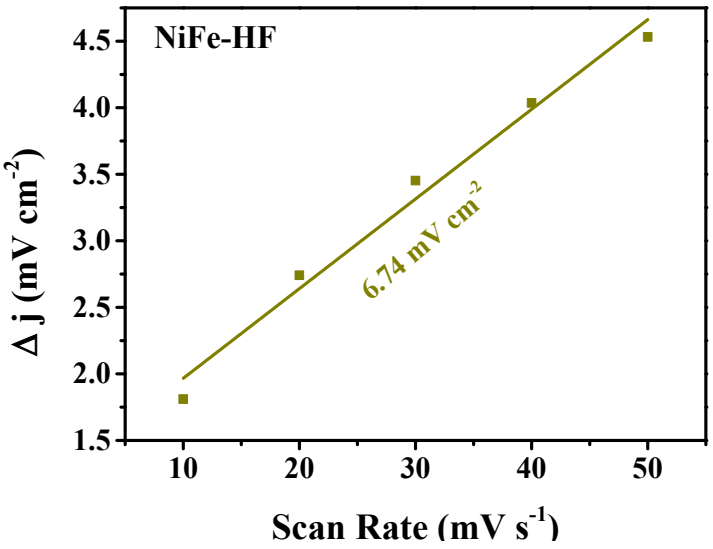

Fig. S23 Current density (at 1.16 V vs RHE) as function of scan rate for NiFe-HF.

Table S1. The ECSA of as-prepared catalysts.

	$NiFe_x$@$NiFe_2O_4$@NC	$NiFe_x$@NC	$NiFe_2O_4$	NiFe-HF
ECSA	4.81	0.93	1.97	1.3

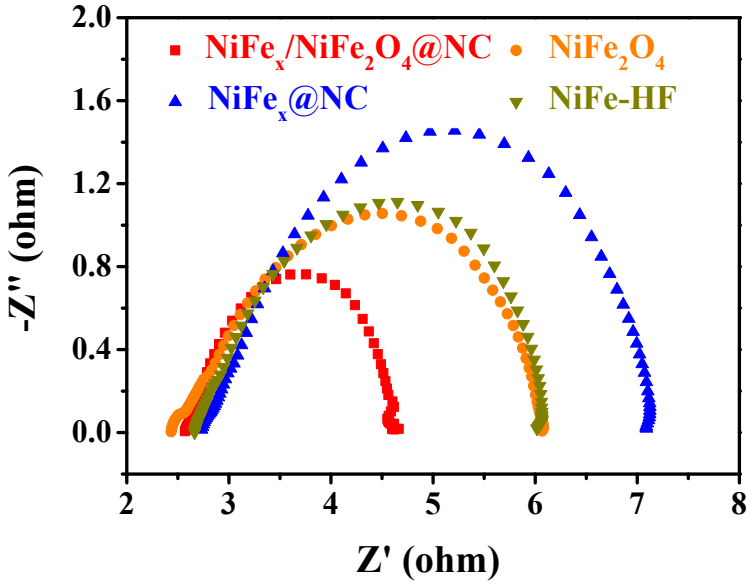

Fig. S24 Nyquist plots of $NiFe_x/NiFe_2O_4$@NC, $NiFe_x$@NC, $NiFe_2O_4$ and NiFe-HF.

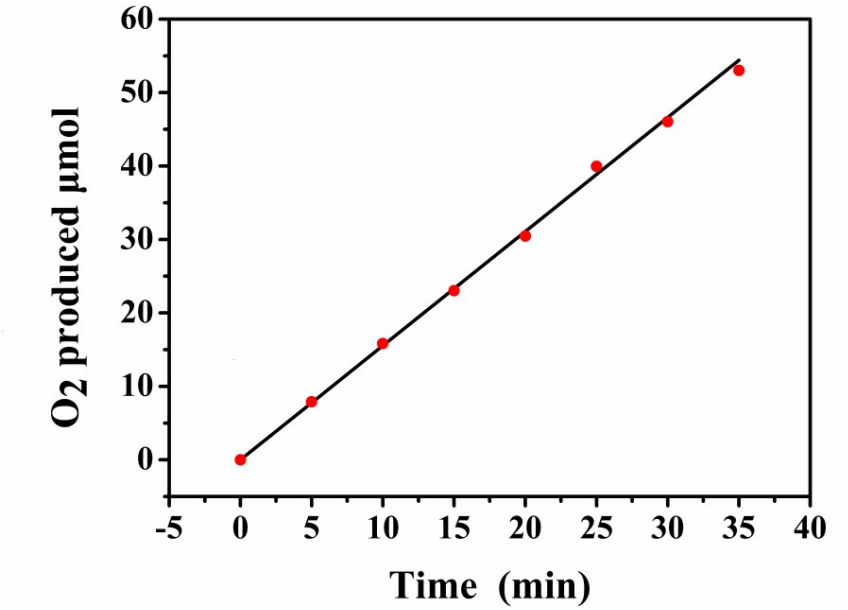

Fig. S25 Faradaic efficiency plot of $NiFe_x@NiFe_2O_4@NC$.

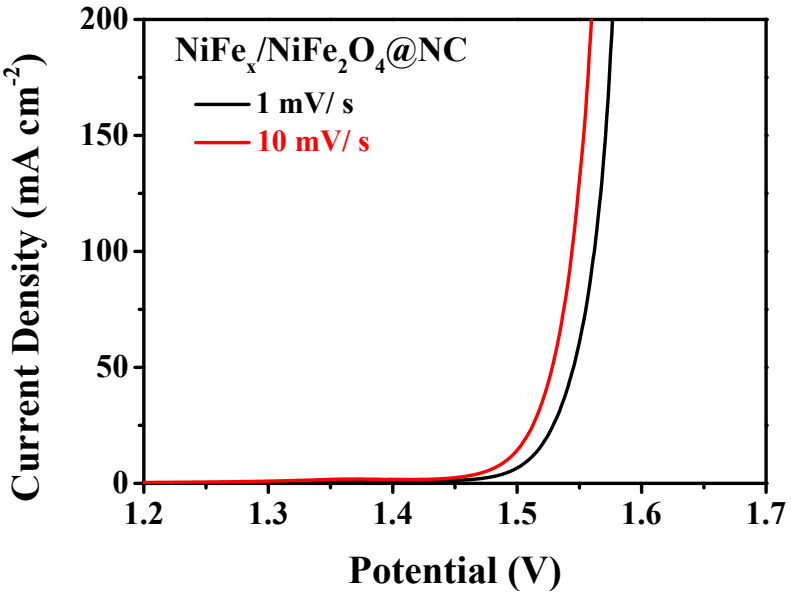

Fig. S26 LSV curves of $NiFe_x/NiFe_2O_4@NC$ at different scan rates.

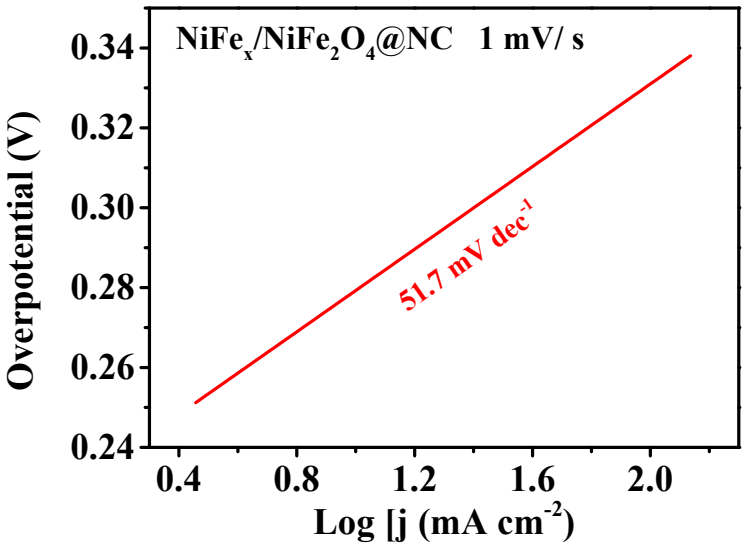

Fig. S27 Tafel plot of $NiFe_x/NiFe_2O_4$@NC at a scan rate of 1 mv/ s.

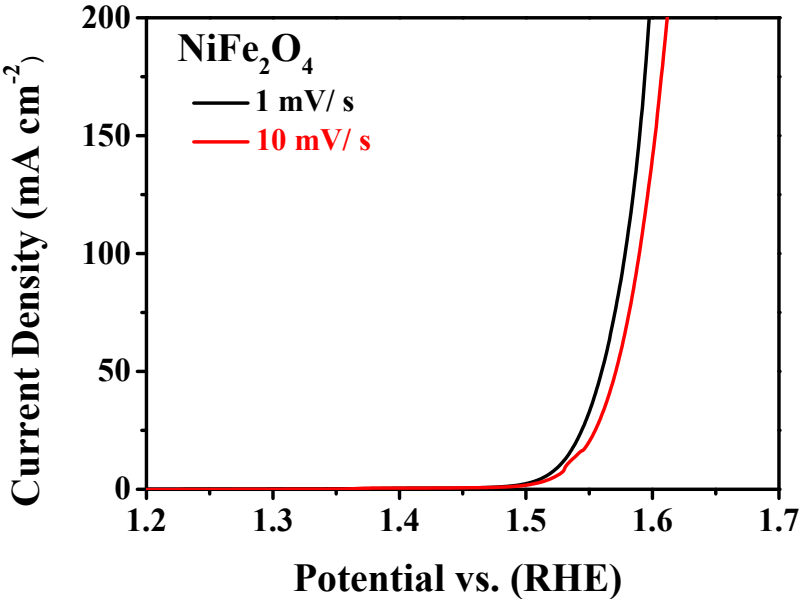

Fig. S28 LSV curves of $NiFe_2O_4$ at different scan rates.

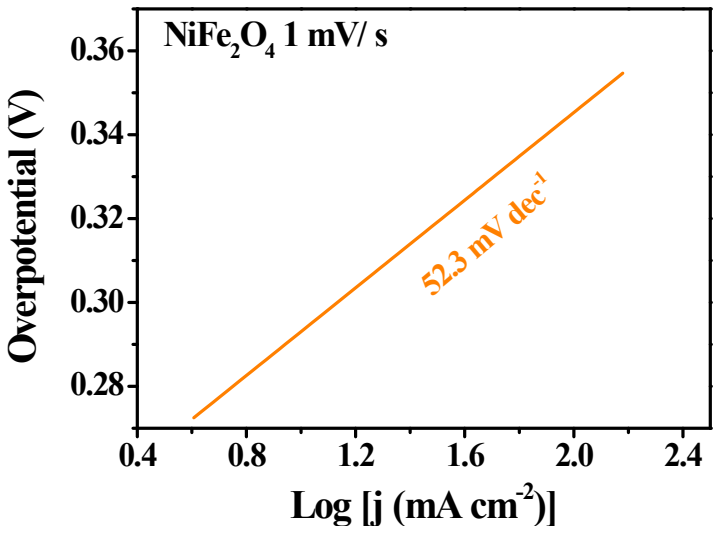

Fig. S29 Tafel plot of $NiFe_2O_4$ at a scan rate of 1 mv/ s.

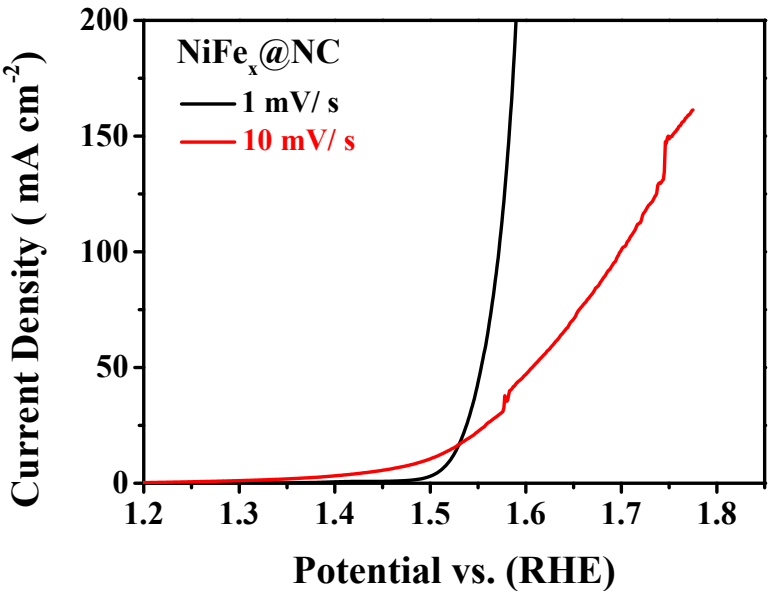

Fig. S30 LSV curves of $NiFe_x$@NC at different scan rates.

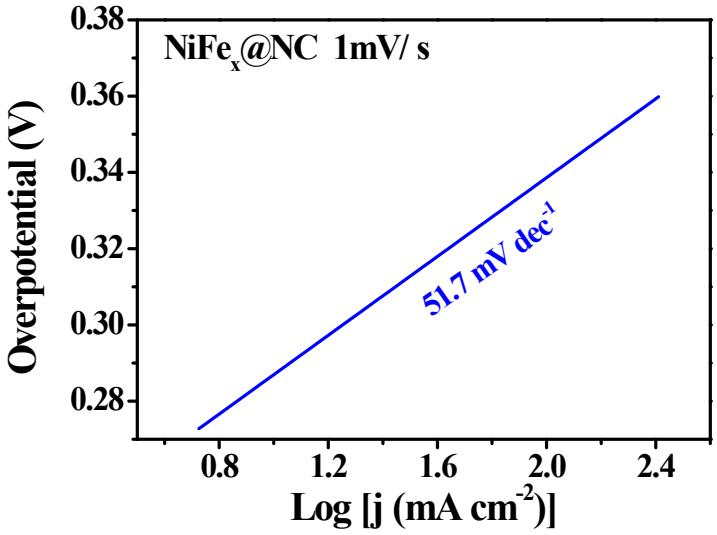

Fig. S31 Tafel plot of NiFe$_x$@NC at a scan rate of 1 mv/ s.

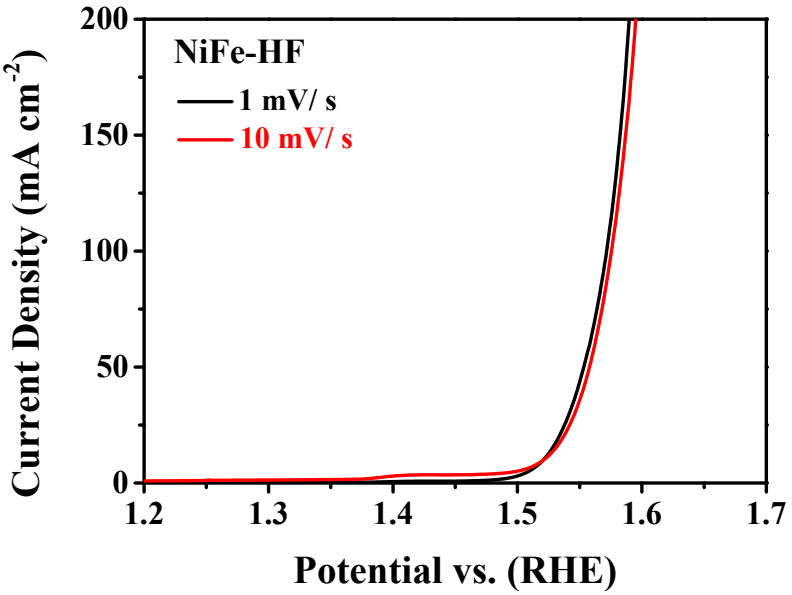

Fig. S32 LSV curves of NiFe-HF at different scan rates.

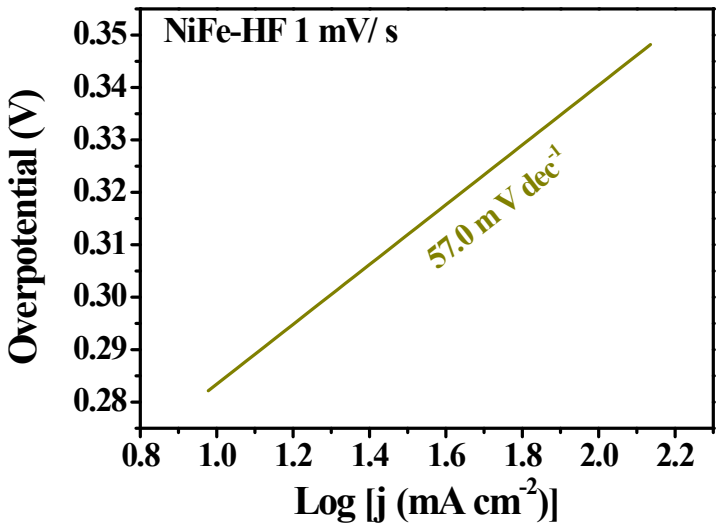

Fig. S33 Tafel plot of NiFe-HF at a scan rate of 1 mv/ s.

Table S2. Comparison of overpotentials of the as-prepared catalysts at different scan rates.

Scan rate	$NiFe_x/NiFe_2O_4$@NC (mV)	$NiFe_2O_4$ (mV)	$NiFe_x$@NC (mV)	NiFe-HF (mV)
1 mV/ s	278	297	281	281
10 mV/ s	262	302	266	282

Table S3. Comparison of Tafel slopes of the as-prepared catalysts at different scan rates.

Scan rate	$NiFe_x/NiFe_2O_4$@NC (mV dec^{-1})	$NiFe_2O_4$ (mV dec^{-1})	$NiFe_x$@NC (mV dec^{-1})	NiFe-HF (mV dec^{-1})
1 mV/ s	51.7	52.3	51.7	57.0
10 mV/ s	51.4	53.6	156	56.7

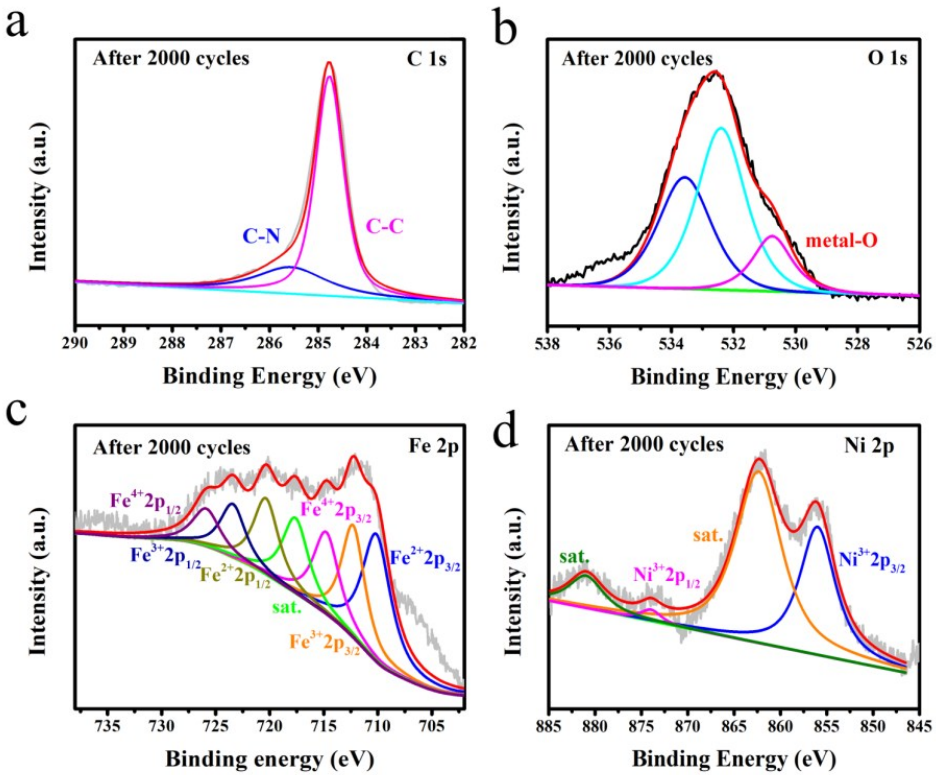

Fig. S34 XPS C 1s (a), O 1s (b), Fe 2p (c), Ni 2p (d) spectra of $NiFe_x/NiFe_2O_4$@NC after 2000 cycles.

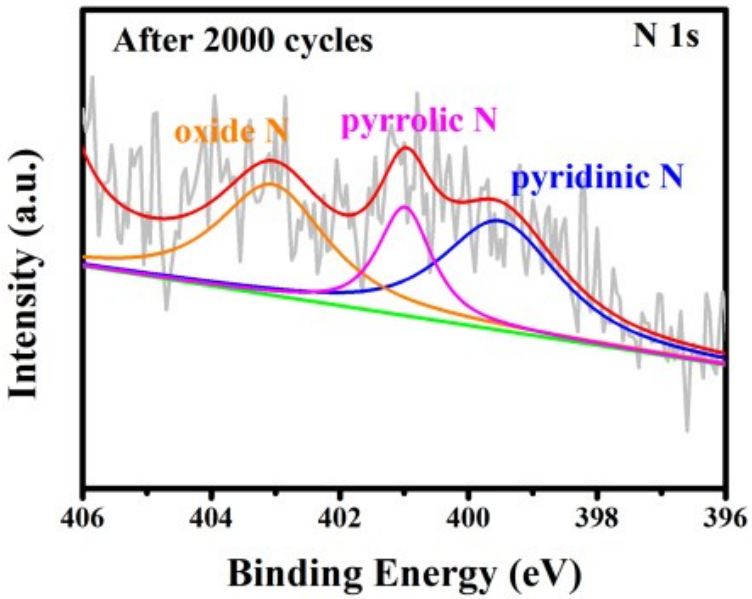

Fig. S35 XPS N 1s spectrum of $NiFe_x/NiFe_2O_4$@NC after 2000 cycles.

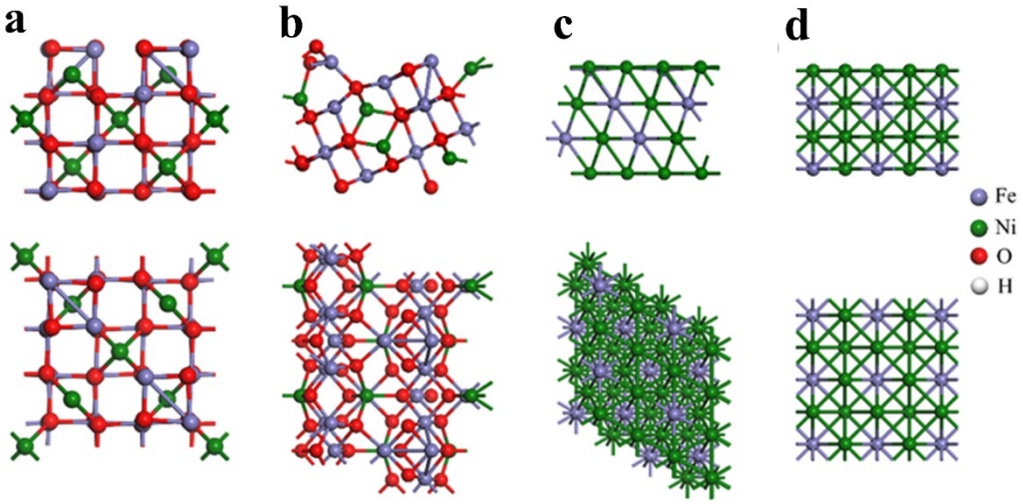

Fig. S36 Side (up) and top (down) view of the geometry of (a) $NiFe_2O_4$ (400), (b) (311), (c) $FeNi_3$ (111) and (d) (200) surface.

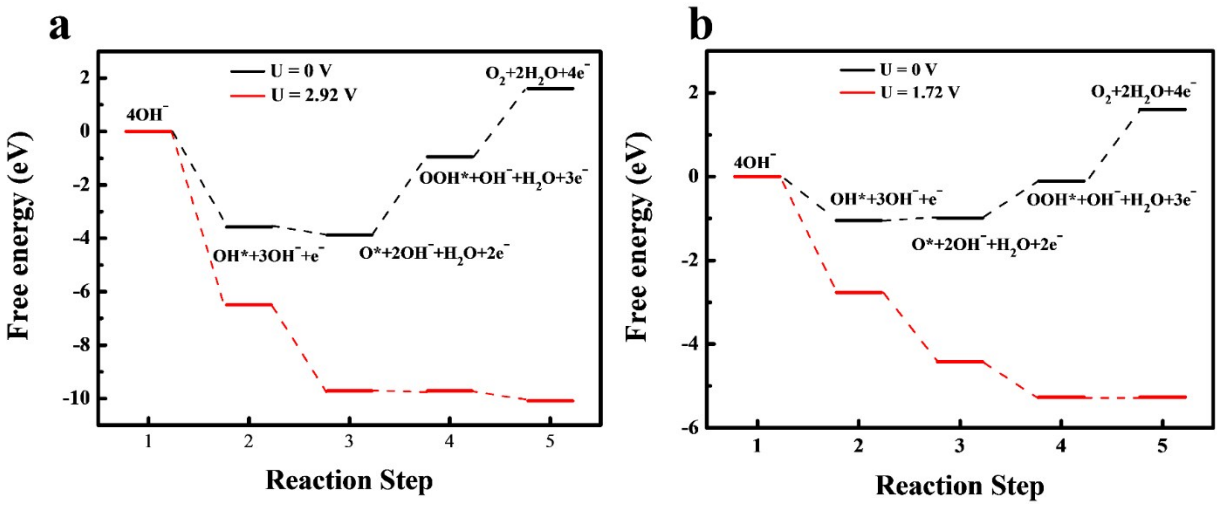

Fig. S37 Free energy diagram for OER on (a) $NiFe_2O_4$ (400) and (b) (311) surfaces at different electrode potentials in alkaline media

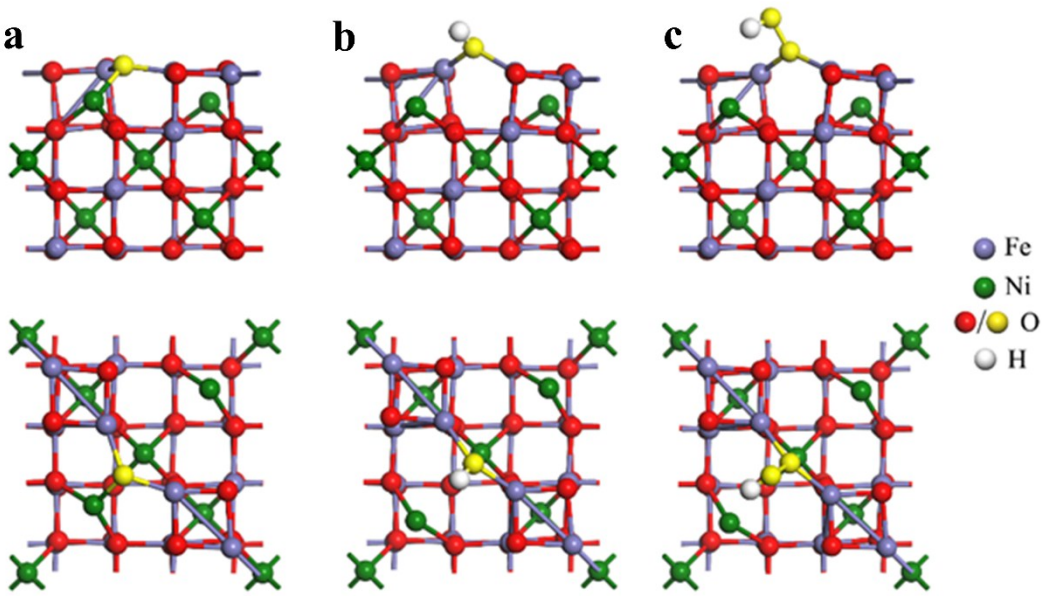

Fig. S38 Side (up) and top (down) view of $NiFe_2O_4$ (400) after the adsorption of (a) O*, (b) OH* and (c) OOH*.

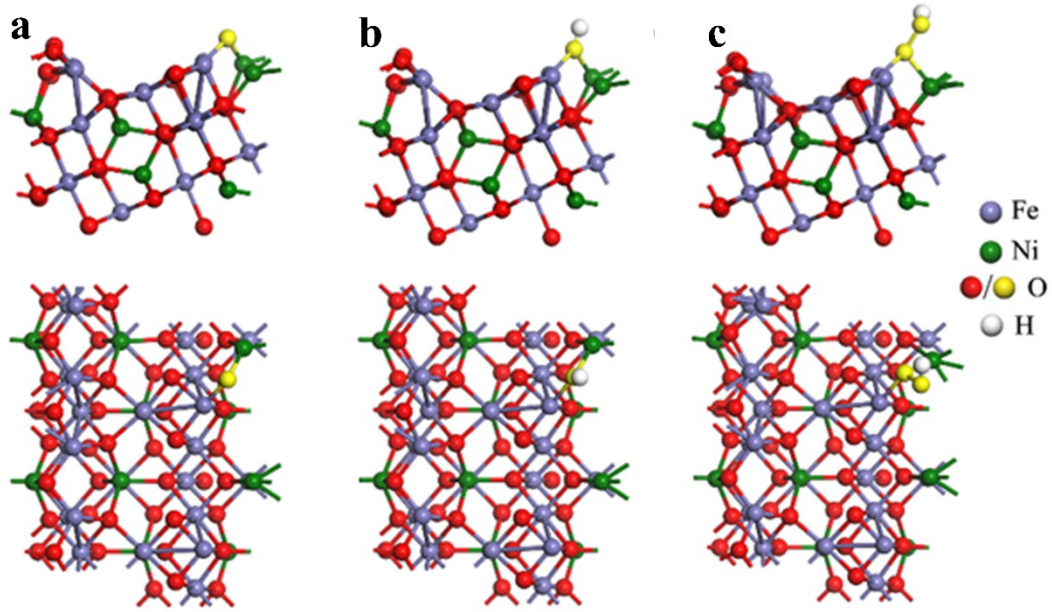

Fig. S39 Side (up) and top (down) view of $NiFe_2O_4$ (311) after the adsorption of (a) O*, (b) OH* and (c) OOH*.

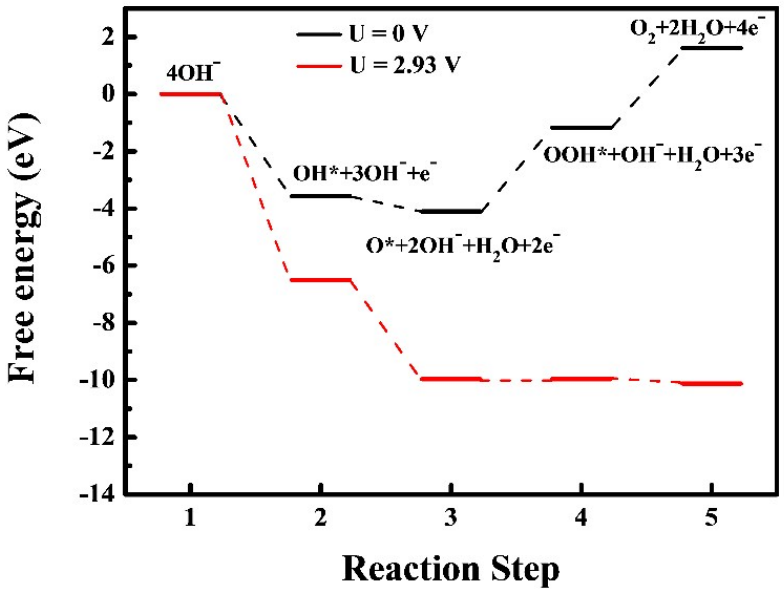

Fig. S40 Free energy diagram for OER on $FeNi_3$ (200) surface at different electrode potentials in alkaline media.

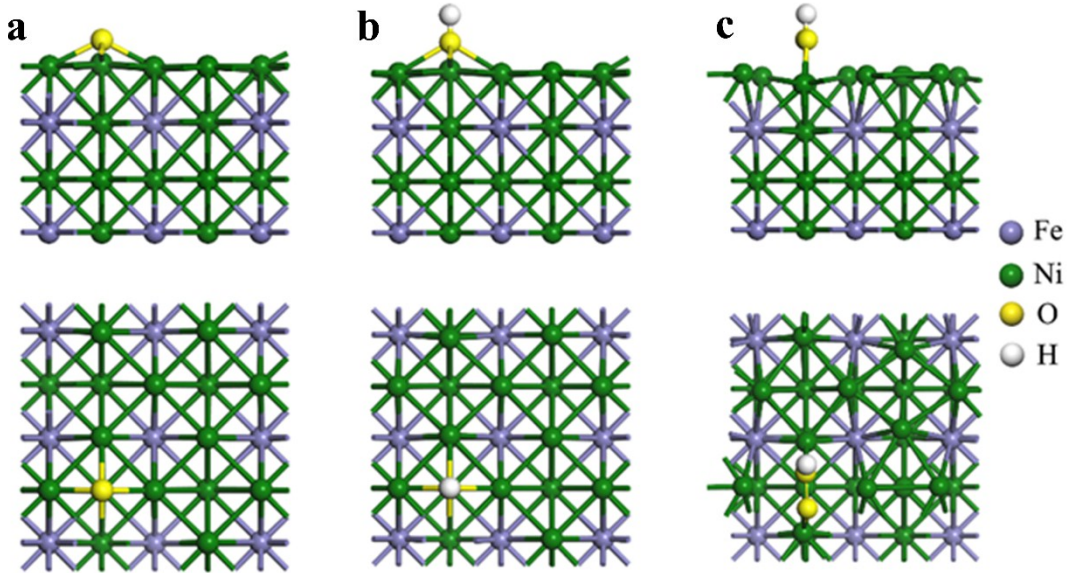

Fig. S41 Side (up) and top (down) view of $FeNi_3$ (200) after the adsorption of (a) O*, (b) OH* and (c) OOH*.

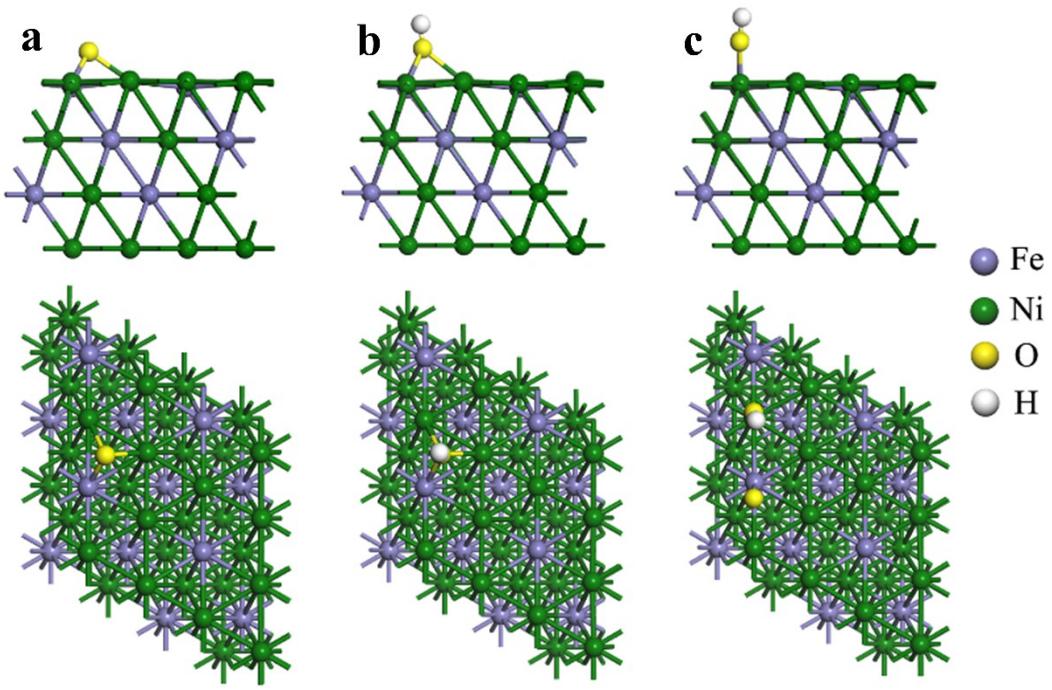

Fig. S42 Side (up) and top (down) view of $FeNi_3$ (111) after the adsorption of (a) O*, (b) OH* and (c) OOH*.

Table S4 Comparison of OER performance of $NiFe_x/NiFe_2O_4$@NC with other reported non-precious metal electrocatalysts tested under similar conditions.

Material	Electrolyte	Current Density ($mA\ cm^{-2}$)	Overpotential (mV)	Stability (h)	C_{dl} ($mF\ cm^{-2}$)	Tafel slope ($mV\ dec^{-1}$)
$NiFe_x/NiFe_2O_4$@NC this work	**1 M KOH**	**10**	**262**	**150**	**24.93**	**51.4**
NiO/NiFe LDH [1]	**1 M KOH**	**10**	**215**	**10**	**—**	**32**
Fe-Ni@NC-CNTs [2]	**1 M KOH**	**10**	**274**	**11**	**12.34**	**45.47**
NiFe LDH@NiCoP/NF [3]	**1 M KOH**	**10**	**220**	**100**	**18.07**	**48.6**
Two cycle $NiFeO_x$/CFP [4]	**1 M KOH**	**10**	**200**	**100**	**—**	**31.5**
NiFe NCs [5]	**1 M KOH**	**10**	**271**	**18**	**16.3**	**48**
Ni_2Fe_1 nanofoams [6]	**1 M KOH**	**10**	**270**	**12**	**0.34**	**70**
P-Ni $_{0.5}$ Fe@C [7]	**1M KOH**	**10**	**256**	**15**	**7.9**	**65**
P-$NiFe_2O_4$ nanosheet [8]	**1 M KOH**	**10**	**231**	**50**	**26.5**	**49**
Fe-Ni-O_x [9]	**0.1 M KOH**	**10**	**584**	**1.7**	**3.82**	**72**
$NiFeO_x$(Fe)/NF-2 [10]	**0.1 M KOH**	**10**	**260**	**12**	**2.47**	**41**
hcp-NiFe@NC [11]	**1 M KOH**	**10**	**226**	**35**	**—**	**41**
NiFe/$NiFeO_x$(0.1) [12]	**0.1 M KOH**	**10**	**340**	**—**	**—**	**34**
FeB_2 [13]	**1 M KOH**	**10**	**296**	**48**	**33.68**	**52.4**
Ni–Fe–O–P [14]	**1 M KOH**	**10**	**227**	**10**		**50**
NiFe-OH NS/NF [15]	**1 M KOH**	**50**	**244**	**30**	**5.145**	**46.7**
LaNiFe hydroxide [16]	**1 M KOH**	**10**	**189**	**100**	**—**	**36**
NiFe/MoS_2 sheet [17]	**1 M KOH**	**10**	**260**	**24**	**4.61**	**48**
Mo-doped Ni–Fe oxide [18]	**1 M KOH**	**10**	**231**	**16**	**—**	**39**
$FeNi_3$@c-2% [19]	**1 M KOH**	**10**	**275**	**10**	**6.8**	**62**
$FeNi_3/NiFeO_x$ [20]	**1 M KOH**	**10**	**246**	**1.67**	**0.0551**	**—**

References

1. Z. W. Gao, J. Y. Liu, X. M. Chen, X. L. Zheng, J. Mao, H. Liu, T. Ma, L. Li, W. C. Wang and X. W. Du, *Adv. Mater.*, 2019, **31**, 1804769–1804777.
2. X. Zhao, P. Pachfule, S. Li, J. R. J. Simke, J. Schmidt and A. Thomas, *Angew. Chem., Int. Ed.,* 2018, **57**, 8921–8926.
3. H. Zhang, X. Li, A. Hähnel, V. Naumann, C. Lin, S. Azimi, S. L. Schweizer, A. W.

Maijenburg and R. B. Wehrspohn, *Adv. Funct. Mater.,* 2018, **28**, 1706847–1706857.
4. H. Wang, H. W. Lee, Y. Deng, Z. Lu, P. C. Hsu, Y. Liu, D. Lin and Y. Cui, *Nat. Commun*., 2015, **6**, 7261–7269.
5. A. Kumar and S. Bhattacharyya, *ACS Appl. Mater. Interfaces*, 2017, **9**, 41906–41915.
6. S. Fu, J. Song, C. Zhu, G.-L. Xu, K. Amine, C. Sun, X. Li, M. H. Engelhard, D. Du and Y. Lin, *Nano Energy*, 2018, **44**, 319–326.
7. A. Fan, C. Qin, X. Zhang, X. Dai, Z. Dong, C. Luan, L. Yu, J. Ge and F. Gao, *ACS Sustain. Chem. Eng.,* 2018, **7**, 2285–2295.
8. Q. Chen, R. Wang, F. Lu, X. Kuang, Y. Tong and X. Lu, *ACS Omega*, 2019, **4**, 3493–3499.
9. J. Jiang, C. Zhang and L. Ai, *Electrochim. Acta*, 2016, **208**, 17–24.
10. X. Shang, Z. Z. Liu, J. Q. Zhang, B. Dong, Y. L. Zhou, J. F. Qin, L. Wang, Y. M. Chai and C. G. Liu, *ACS Appl. Mater. Interfaces*, 2018, **10**, 42217–42224.
11. C. Wang, H. Yang, Y. Zhang and Q. Wang, *Angew. Chem., Int. Ed.,* 2019, **58**, 6099–6103.
12. K. Zhu, M. Li, X. Li, X. Zhu, J. Wang and W. Yang, *Chem. Commun.*, 2016, **52**, 11803–11806.
13. H. Li, P. Wen, Q. Li, C. Dun, J. Xing, C. Lu, S. Adhikari, L. Jiang, D. L. Carroll and S. M. Geyer, *Adv. Energy Mater.,* 2017, **7,** 1700513–1700525.
14. C. Xuan, J. Wang, W. Xia, J. Zhu, Z. Peng, K. Xia, W. Xiao, Huolin L. Xin and D. Wang, *J. Mater. Chem. A*, 2018, **6**, 7062–7069.
15. W. Zhu, T. Zhang, Y. Zhang, Z. Yue, Y. Li, R. Wang, Y. Ji, X. Sun and J. Wang, *Appl. Catal. B: Environ.,* 2019, **244**, 844–852.
16. G. Chen, Y. Zhu, H. M. Chen, Z. Hu, S. F. Hung, N. Ma, J. Dai, H. J. Lin, C. T. Chen, W. Zhou and Z. Shao, *Adv. Mater.*, 2019, **31**, 1900883–1900890.
17. Y. Wang, Y. Zhou, M. Han, Y. Xi, H. You, X. Hao, Z. Li, J. Zhou, D. Song, D. Wang and F. Gao, *Small*, 2019, **15**, 1805435–1805443.
18. Y. Chen, C. Dong, J. Zhang, C. Zhang and Z. Zhang, *J. Mater. Chem. A*., 2018, **6**, 8430–8440.
19. H. Fan, H. Yu, Y. Zhang, Y. Zheng, Y. Luo, Z. Dai, B. Li, Y. Zong and Q. Yan, *Angew. Chem., Int. Ed.,* 2017, **56**, 12566–12570.
20. X. Yan, L. Tian, K. Li, S. Atkins, H. Zhao, J. Murowchick, L. Liu and X. Chen, *Adv. Mater. Interfaces*, 2016, **3**, 1600368–1600376.